Available online at www.sciencedirect.com
SCIENCE DIRECT®
Journal of Solid State Chemistry 170 (2003) 289–293
JOURNAL OF SOLID STATE CHEMISTRY
http://elsevier.com/locate/jssc

Efficient UV-emitting X-ray phosphors: octahedral $Zr(PO_4)_6$ luminescence centers in potassium hafnium–zirconium phosphates $K_2Hf_{1-x}Zr_x(PO_4)_2$ and $KHf_{2(1-x)}Zr_{2x}(PO_4)_3$

C.C. Torardi,[a,*] C.R. Miao,[a] and J. Li[b]

[a] DuPont Central Research and Development Experimental Station, Wilmington, DE 19880-0356, USA
[b] Department of Chemistry, Rutgers University, Camden, NJ 08102, USA

Received 24 May 2002; received in revised form 23 September 2002; accepted 15 October 2002

Abstract

Potassium hafnium–zirconium phosphates, $K_2Hf_{1-x}Zr_x(PO_4)_2$ and $KHf_{2(1-x)}Zr_{2x}(PO_4)_3$, are broad-band UV-emitting phosphors. At room temperature, they have emission peak maxima at approximately 322 and 305 nm, respectively, under 30 kV peak molybdenum X-ray excitation. Both phosphors demonstrate luminescence efficiencies that make them up to ~60% as bright as commercially available $CaWO_4$ Hi-Plus. The solid-state and flux synthesis conditions, and X-ray excited UV luminescence of these two phosphors are discussed. Even though the two compounds have different atomic structures, they contain zirconium in the same active luminescence environment as that found in highly efficient UV-emitting $BaHf_{1-x}Zr_x(PO_4)_2$. All the three materials have hafnium and zirconium in octahedral coordination via oxygen-atom corner sharing with six separate PO_4 tetrahedra. This octahedral $Zr(PO_4)_6$ moiety appears to be an important structural element for efficient X-ray excited luminescence, as are the edge-sharing octahedral TaO_6 chains for tantalate emission.

Keywords: Potassium hafnium–zirconium phosphate; Zirconium luminescence; Tantalum luminescence; X-ray phosphor; UV emission

1. Introduction

For conventional medical X-ray imaging applications [1,2], there has been interest in replacing visible-light-emitting phosphors with UV-emitting phosphors that significantly improve the sharpness of the radiographic image [3,4]. The emitted UV light is highly attenuated within the phosphor-intensifying screen, resulting in sharper images than those obtained using visible-light-emitting screens. Also, the UV light emitted from the screen is more efficiently absorbed by the silver halide emulsion, and any remaining UV light transmitted through the emulsion is attenuated by the film base, thereby eliminating "print-through".

Attention has been given to hafnium-oxide-based phosphors because HfO_2 and hafnate compounds have good X-ray absorption and can emit in the UV region when doped with zirconium. As an example, we recently reported the synthesis, structure, chemistry, and luminescence of a highly efficient UV-emitting X-ray phosphor, $BaHf_{1-x}Zr_x(PO_4)_2$ ($x = 0-0.2$) [5].

Here, we discuss two other UV-emitting hafnium-phosphate phosphors that were discovered in the course of our research. These compounds are important because they provide insight on how crystal structure influences luminescence. A structural comparison reveals that the three phosphates, i.e., the barium and two potassium compounds, contain the same chemical and structural environment around the luminescent zirconium centers.

Developing an understanding of the relationship between structure and luminescence is of practical, as well as theoretical, importance in the design and synthesis of new phosphor compounds. Knowing what structural features should be incorporated into a material in order to give luminescence at a specific wavelength or region of wavelengths is extremely valuable. As an example, we note here a structural commonality among several efficient tantalum-oxide-

*Corresponding author. Fax: +302-695-1664.
E-mail address: charlie.c.torardi@usa.dupont.com (C.C. Torardi).

0022-4596/03/$ - see front matter © 2002 Elsevier Science (USA). All rights reserved.
PII: S0022-4596(02)00087-7

based phosphors. Earlier, we described the existence of edge-sharing chains of TaO_6 distorted octahedra in M′-$YTaO_4$ [2] (M′ is the low-temperature monoclinic form), and edge-sharing chains of TaO_6 octahedra in $Li_3Ta_{1-x}Nb_xO_4$ [6]. We find similar chains [7] in the high-temperature monoclinic structure M-$YTaO_4$ [8] and in $Zn_3Ta_2O_8$ [9]. The X-ray excited luminescence efficiency of M-$YTaO_4$ was reported [3] as being about one-half that of M′-$YTaO_4$, and the difference was attributed to a more efficient charge-transfer process for the M′ structure. However, when M-$YTaO_4$ is synthesized to yield the proper crystallite size, it is equal in efficiency to the M′ modification [7]. The TaO_6 chains behave in a very similar manner in regard to luminescence in the two compounds. Therefore, in these four materials, edge-sharing TaO_6 chains provide a significant structural condition that allows efficient luminescence to occur.

The structure–luminescence study described in this paper for hafnium–zirconium phosphates reveals yet another phosphor-building block.

2. Experimental

2.1. Synthesis and characterization

$K_2Hf_{1-x}Zr_x(PO_4)_2$ ($x = 0-1$) compositions were prepared using stoichiometric quantities of KH_2PO_4 (99.8%, J.T. Baker), HfO_2 (99%, Alfa-Aesar, containing ~1–2 wt% zirconium), and ZrO_2 (99.9975%, Johnson-Matthey). The components were ground in an agate mortar and fired in an alumina crucible in air, ramping up to 1200°C in 6 h, soaking for 12 h, then allowing the furnace to cool with the power removed. One sample ($x = 0.03$) was made at 1100°C, and several compositions ($x = 0-0.05$) were also prepared at 1100°C using a flux. For these samples, 10% by weight of K_2SO_4 (99.998%, Alfa-Aesar) was added to the reaction mixture before grinding. The flux products were washed thoroughly with deionized water and dried under an infrared lamp.

$KHf_{2(1-x)}Zr_{2x}(PO_4)_3$ ($x = 0-1$) compositions were prepared without flux in the same manner except that $(NH_4)H_2PO_4$ (99.95%, J.T. Baker) was included as a source of phosphate.

The amount of Zr present in the 99%-pure HfO_2 was ignored in calculating the quantity of ZrO_2 required for any x value. For example, a preparation designed to have $x = 0$ used 99%-pure HfO_2 and no ZrO_2.

X-ray powder diffraction (Philips APD3720 or X'Pert PW/3040 with Cu radiation) was used to verify phase purity. No pattern for $K_2Hf(PO_4)_2$ is given in the JCPDS-ICDD database. However, for $K_2Hf_{1-x}Zr_x(PO_4)_2$ ($x = 0-1$), the patterns showed the line positions of isostructural $K_2Zr(PO_4)_2$ (JCPDS-ICDD card no. 76-242) and often included a small amount of $KHf_{2(1-x)}Zr_{2x}(PO_4)_3$ impurity (estimated to be <5% from a comparison of the intensities of the strongest lines), which has the same pattern as $KHf_2(PO_4)_3$ and $KZr_2(PO_4)_3$ (JCPDS-ICDD card nos. 38-1471 and 35-756, respectively).

The XPD patterns for $KHf_{2(1-x)}Zr_{2x}(PO_4)_3$ ($x = 0-1$) were the same as those of the isostructural compounds $KHf_2(PO_4)_3$ and $KZr_2(PO_4)_3$ (JCPDS-ICDD card nos. as above) and frequently showed a small amount (<5%) of $Hf_{1-x}Zr_xP_2O_7$ impurity, which has the same pattern as HfP_2O_7 and ZrP_2O_7 (JCPDS-ICDD card nos. 37-1494 and 49-1079, respectively).

For both structure types, the observed impurity levels did not significantly affect the X-ray excited emission peak shape or intensity. Particle size and morphology were examined using scanning electron microscopy.

2.2. X-ray luminescence measurements

For measurements of X-ray stimulated luminescence properties, the powders were first mixed with a polymeric binder and coated on a sheet of base material. This technique for making a phosphor "screen" is similar to that used in commercial production, and permits the preparation of a screen with a uniform thickness of uniformly dense material. A cardboard base material and carboxylated methyl methacrylate acrylic binder were chosen to avoid interference with the X-ray luminescence measurements.

The X-ray luminescence of the samples was examined under ambient conditions using a molybdenum X-ray source operating at 30 kV (peak voltage) and 10 mA. The sample was exposed to polychromatic X-radiation, and two detectors were used to measure the luminescence properties [2]. The first detection system consisted of a Hamamatsu R928 photomultiplier and a picoammeter, and was used to measure the total intensity of light coming from the sample, or the overall X-ray-to-light conversion efficiency (i.e., the "speed"). This speed was compared relative to that of a $CaWO_4$ Hi-Plus industry standard. The second detection system used a SPEX 500M spectrometer, in which the light from the sample passes through a 0.5 m monochromator before entering a Hamamatsu R928 photomultiplier. Using this detection system, a characteristic spectrum of the luminescence of the sample could be obtained by scanning through the range of detectable wavelengths allowed by the monochromator, and measuring the intensity of light at each interval. The Hamamatsu photomultipliers were selected because of their relatively flat response in the region 300–600 nm.

3. Results and discussion

3.1. Synthesis and characterization

The 99%-grade hafnia, typically containing ~1–2 wt% zirconium (metals basis), was used because of its relatively low cost (a significant consideration for commercial use). These levels of zirconium in hafnia result in a Zr/Hf mole ratio of ~0.03. In our studies, the amount of Zr in 99%-pure HfO_2 was ignored in calculating the quantities of ZrO_2 required for any x value, and the reported x values are, therefore, considered only nominal values. The actual zirconium content of the phosphor is higher. Note, therefore, that the emission intensity at any nominal value of x reported in this paper for $K_2Hf_{1-x}Zr_x(PO_4)_2$ and $KHf_{2(1-x)}Zr_{2x}(PO_4)_3$ will vary with the zirconium content of the HfO_2 starting material. Other impurities, such as iron, in the hafnium oxide may also affect the intensity.

A suitable reaction temperature range for both phosphor materials is 1100–1200°C. For $K_2Hf_{1-x}Zr_x(PO_4)_2$, several K_2SO_4 flux reactions were performed to study the morphological influence on luminescence. After hand-grinding in a mortar, SEM images showed the 1100°C no-flux product to consist of large, irregularly shaped agglomerates, whereas the 1100°C flux product contained thick, rough-edged polycrystalline plates. However, there was no advantage in using the flux in the synthesis, either in terms of phase purity or luminescence efficiency (discussed below), as also observed in the synthesis of $BaHf_{1-x}Zr_x(PO_4)_2$ [5].

For $KHf_{2(1-x)}Zr_{2x}(PO_4)_3$, one K_2SO_4 flux reaction was attempted, but the product was highly contaminated with the potassium-rich compound, as expected, so the $KHf_{2(1-x)}Zr_{2x}(PO_4)_3$ compositions were made without flux.

3.2. Structures

The crystal structure of $K_2Hf(PO_4)_2$ is essentially identical to that of $K_2Zr(PO_4)_2$ [10]. The hafnium compound is trigonal, $P\bar{3}$ with $a = 5.2$ Å, $c = 9.0$ Å and an estimated density of 3.6 g/cm^3. By analogy with the reported single-crystal structure of $K_2Zr(PO_4)_2$ [10], the hafnium structure contains hafnium in octahedral coordination with oxygen atoms from six separate phosphate groups. The hafnium phosphate octahedra are interconnected in two dimensions to form layers. Potassium ions, located between the layers, are seven-coordinated to oxygen atoms. The layered structure of $K_2Hf(PO_4)_2$ bears strong relationships to that of the efficient UV-emitting (356 nm) X-ray phosphor, $BaHf_{1-x}Zr_x(PO_4)_2$ [5], especially in regard to the HfO_6–PO_4 connectivity.

$KHf_2(PO_4)_3$ has a structure essentially identical to that of $KZr_2(PO_4)_3$ [11] and is rhombohedral, $R\bar{3}c$ (hexagonal) with $a = 8.7$ Å, $c = 23.9$ Å and an estimated density of 4.3 g/cm^3. By analogy with $KZr_2(PO_4)_3$ [11], the hafnium structure contains hafnium in octahedral coordination with oxygen atoms from six separate phosphate groups, an environment that also occurs for hafnium in $K_2Hf(PO_4)_2$ (described above) and $BaHf_{1-x}Zr_x(PO_4)_2$ [5]. Each oxygen atom of the phosphate tetrahedron is shared with a separate hafnium atom, and as a result, a three-dimensional, rather than layered, structure is formed. Potassium ions are six-coordinated to oxygen atoms in a trigonal antiprism.

The three efficient UV-emitting X-ray phosphors, $K_2Hf_{1-x}Zr_x(PO_4)_2$, $KHf_{2(1-x)}Zr_{2x}(PO_4)_3$, and $BaHf_{1-x}Zr_x(PO_4)_2$, have the common structural feature of each hafnium and zirconium ion bonded to six separate phosphate tetrahedra (e.g., see Fig. 1, and Ref. [5, Fig. 1]). This atomic arrangement, i.e., $Zr(PO_4)_6$, creates a luminescence-active center for zirconium.

3.3. X-ray excited luminescence

The X-ray excited emission spectra of $K_2Hf_{1-x}Zr_x(PO_4)_2$ with nominal x values of 0.0–1.0 are all similar. Broad band emission occurs in the UV at 320–325 nm. The peak starts to shift from 320 to 325 nm at $x \sim 0.7$, but no significant change in the peak width is observed. As representative examples, the $x = 0.03$ and 1.0 emission spectra are given in Fig. 2. Although it is not obvious from the figure, the second-order peaks occurring at twice the wavelength indicate that emission is coming from two different energy levels. The peaks in Fig. 2 consist predominantly of emission at 320–325 nm,

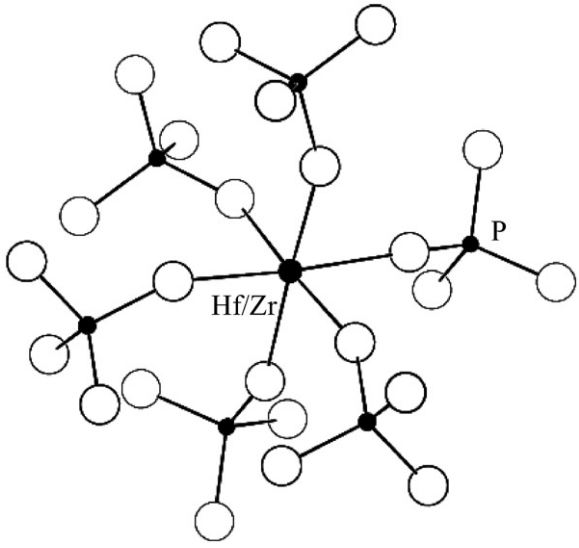

Fig. 1. The Hf/Zr$(PO_4)_6$ unit in the X-ray excited UV-emitting phosphors $KHf_{2(1-x)}Zr_{2x}(PO_4)_3$ ($x = 0-1$).

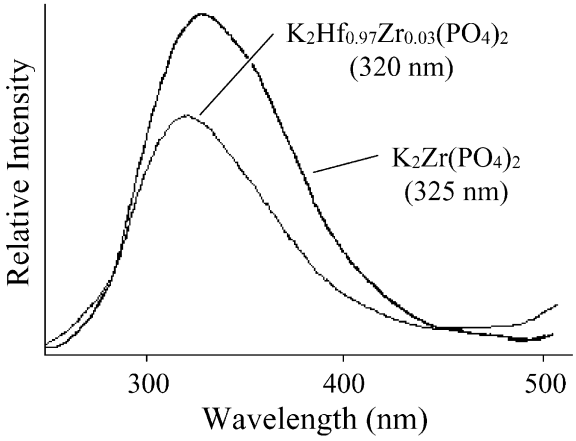

Fig. 2. X-ray excited UV-emission spectra of $K_2Hf_{1-x}Zr_x(PO_4)_2$ having nominal values $x = 0.03$ (see text) and $x = 1.0$.

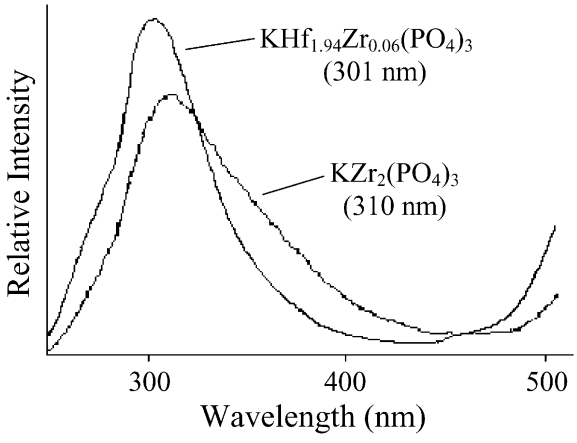

Fig. 4. X-ray excited UV-emission spectra of $KHf_{2(1-x)}Zr_{2x}(PO_4)_3$ having nominal values $x = 0.03$ (see text) and $x = 1.0$.

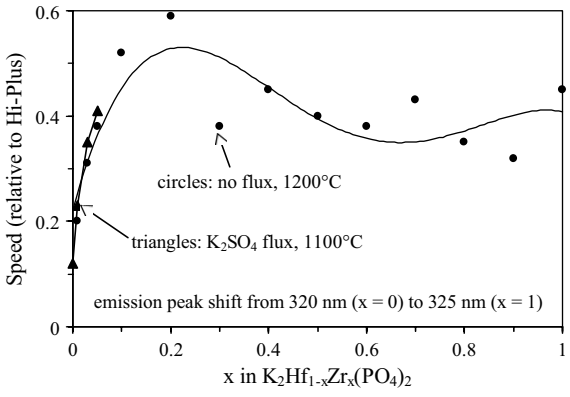

Fig. 3. Luminescence efficiency (speed) of X-ray excited $K_2Hf_{1-x}Zr_x(PO_4)_2$ having nominal x values from 0.0 to 1.0 (see text). Speed values are relative to a $CaWO_4$ Hi-Plus standard. Flux and solid-state preparations are compared. The solid line is only a guide for the eye.

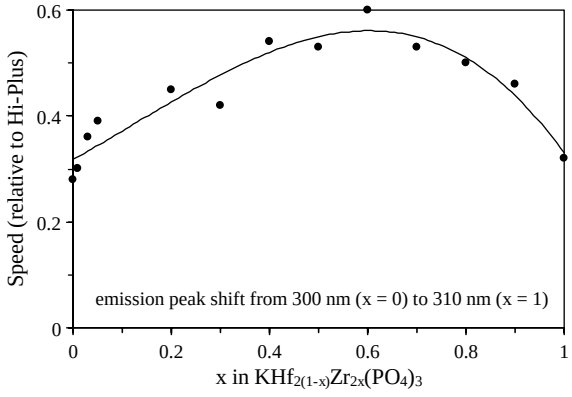

Fig. 5. Luminescence efficiency (speed) of X-ray excited $KHf_{2(1-x)}Zr_{2x}(PO_4)_3$ having nominal x values from 0.0 to 1.0 (see text). Speed values are relative to a $CaWO_4$ Hi-Plus standard. The solid line is only a guide for the eye.

but also contain weaker emission at ~280 nm. Other than small shifts in the average peak position, both peaks appear to be independent of phase purity (e.g., 95% or 99%), method of synthesis (i.e., solid state or flux), and composition (e.g., $x = 0$ or 1). It then seems that two luminescence sites are created by the high-energy excitation, or the method of synthesis produces two kinds of crystallites that differ in their defect chemistry. The more-likely former hypothesis could be investigated by UV excitation experiments to determine the number of emission sites. Clearly, more work is required to understand this phenomenon. The speed, or luminescence efficiency, increases sharply from $x = 0$ to 0.2, to reach a value of ~0.6 relative to $CaWO_4$ Hi-Plus, the latter defined to have a speed of 1.0 (Fig. 3). There is no difference in speed between samples made via solid-state reaction at 1200°C, or K_2SO_4 flux at 1100°C over the range studied, $x = 0-0.05$. From $x = 0.2$ to 1.0, the speed levels off at a value of about 0.4. The scatter of speed values vs x in Fig. 3 may be due to low levels of emission from varying amounts of $KHf_{2(1-x)}Zr_{2x}(PO_4)_3$ impurity (observed in the XPD patterns).

For $KHf_{2(1-x)}Zr_{2x}(PO_4)_3$, the broad-band UV emission shifts steadily from ~300 nm for $x = 0$ to ~310 nm for $x = 1.0$. The peak width increases with x in the region 0.2–1.0. Fig. 4 shows the emission peaks for the compositions having $x = 0.03$ and 1.0. For all values of x, the emission peak is asymmetric with a shoulder on the high-energy side, showing that emission is coming from two different energy levels (note that in Figs. 2 and 4, the upturn of the tails seen at ~500 nm is the onset of the second-order peaks). The broad bands in Fig. 4 consist of emission in the region 300–310 nm, and emission at ~275 nm. As discussed above for $K_2Hf_{1-x}Zr_x(PO_4)_2$, the two emission peaks from $KHf_{2(1-x)}Zr_{2x}(PO_4)_3$ are independent of purity, synthesis method, and composition, and they appear to be in the nature of the material as synthesized and studied.

The speed increases gradually from ~0.3 to ~0.6 $CaWO_4$ Hi-Plus in the region $x = 0-0.6$, then decreases slightly at higher x values (Fig. 5).

In summary, potassium hafnium–zirconium phosphates, $K_2Hf_{1-x}Zr_x(PO_4)_2$ and $KHf_{2(1-x)}Zr_{2x}(PO_4)_3$, are efficient broad-band UV-emitting X-ray phosphors. The UV luminescence is the result of zirconium-to-oxygen charge transfer within the $Zr(PO_4)_6$ subunits. The observed luminescence efficiencies of the two structure types make them ~60% as bright as commercially available $CaWO_4$ Hi-Plus. However, for commercial use, this level of efficiency is not adequate, and the relatively low X-ray absorption (densities less than ~3.6 and 4.3 g/cm^3 for the 2:1 and 1:2 compounds, respectively) is a disadvantage. The two compounds have different crystal structures, but both have zirconium in the same active luminescence environment as that found in highly efficient UV-emitting $BaHf_{1-x}Zr_x(PO_4)_2$ [5]. All the three materials contain hafnium and zirconium in octahedral coordination via oxygen-atom corner sharing with six separate PO_4 tetrahedra. This octahedral $Zr(PO_4)_6$ moiety appears to be an important structural element for efficient X-ray excited luminescence, as are the edge-sharing octahedral TaO_6 chains for tantalate emission.

Acknowledgments

We thank M.K. Crawford for discussions on phosphor materials, B.D. Jones for assistance with the X-ray excitation spectrometer, D.J. Redmond and C.M. Foris for X-ray powder diffraction data, and K.R. Warrington for SEM images. JL would like to acknowledge Rutgers University for FASP support.

References

[1] L.H. Brixner, Mater. Chem. Phys. 16 (1987) 253.
[2] S.L. Issler, C.C. Torardi, J. Alloys Comp. 229 (1995) 54.
[3] L.H. Brixner, H.-y. Chen, J. Electrochem. Soc. 130 (1983) 2435.
[4] J. Beutel, D.J. Mickewich, S.L. Issler, R. Shaw, Phys. Med. Biol. 38 (1993) 1195.
[5] C.R. Miao, C.C. Torardi, J. Solid State Chem. 155 (2000) 229.
[6] C.R. Miao, C.C. Torardi, J. Solid State Chem. 145 (1999) 110.
[7] C.C. Torardi, unpublished results.
[8] G.M. Wolten, Acta Crystallogr. 23 (1967) 939.
[9] S.K. Kurinec, P.D. Rack, M.D. Potter, T.N. Blanton, J. Mater. Res. 15 (2000) 1320.
[10] M. Dörffel, J. Liebertz, Z. Kristallogr. 193 (1990) 155.
[11] M. Sljukic, B. Matkovic, B. Prodic, D. Anderson, Z. Kristallogr. 130 (1969) 148.